

Protocol for Evaluating Anion Exchange Membranes for Nonaqueous Redox Flow Batteries

Jessica L. Tami,^a Md. Motiur R. Mazumder,^b Grace E. Cook,^a Shelley D. Minteer,^{c,d*} and Anne J. McNeil^{a,e,*}

^a Department of Chemistry, University of Michigan, Ann Arbor, Michigan, 48109-1055, United States.

^b Department of Chemistry and Biochemistry, Utah Tech University, St. George, Utah, 84770-3875, United States.

^c Department of Chemistry, Missouri University of Science and Technology, Rolla, Missouri, 65409-6518, United States.

^d Kummer Institute Center for Resource Sustainability, Missouri University of Science and Technology, Rolla, Missouri, 65409-6518, United States.

^e Macromolecular Science and Engineering Program, University of Michigan, Ann Arbor, Michigan, 48109-1055, United States.

Keywords: Anion exchange membranes, redox flow batteries, nonaqueous, crossover, permeability, electrochemical impedance spectroscopy, voltage efficiency

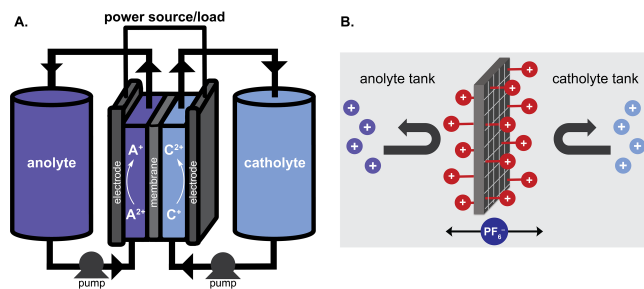
ABSTRACT: Nonaqueous redox flow batteries (NARFBs) often suffer from reduced battery lifetime and decreased coulombic efficiency due to crossover of the redox-active species through the membrane. One method to mitigate this undesired crossover is to judiciously choose a membrane based on several criteria: swelling and structural integrity, size and charge of redox active species, and ionic conductivity. Most research to date has focused on reducing crossover by synthesizing modified redox-active molecules and/or new membranes. However, no standard protocol exists to compare membranes and a comprehensive study comparing membranes has yet to be done. To address both these limitations, we evaluate herein 26 commercial anion exchange membranes (AEMs) to assess their compatibility with common nonaqueous solvents and their resistance to crossover by using neutral and cationic redox-active molecules. Ultimately, we found that all the evaluated AEMs perform poorly in organic solvents due to uncontrolled swelling, low ionic conductivity, and/or high crossover rates. We believe that this method, and the generated data, will be useful to evaluate and compare the performance of all anion exchange membranes—commercial and newly synthesized—and should be implemented as a standard protocol for future research.

INTRODUCTION

Renewable energy can be harvested through several avenues, including solar panels and wind turbines. However, solar and wind energy are intermittent, meaning they are not continuously accessible.¹ A safe, sustainable, and efficient way to store renewable energy is necessary so that it can be employed when needed. A promising technology for energy storage is the redox flow battery (RFB), which has the potential to be used in grid-scale operations.² RFBs consist of an electrochemical flow cell and two reservoirs, one of which contains an anolyte (redox-active species that undergoes reduction upon charging) and the other a catholyte (redox-active species that undergoes oxidation upon charging), both dissolved in a solvent with a supporting electrolyte (Scheme 1A).³ An advantage to RFBs is that power and capacity can be independently scaled. Power is affected by the size of the electrodes (in each cell) and the number of cells whereas capacity is affected by the volume and concentration of redox-active molecules in the reservoirs.⁴ The state-of-the-art commercial RFB is aqueous and uses expensive vanadium compounds for the redox-active molecules

and hazardous sulfuric acid for the supporting electrolyte.^{5,6,7} Additionally, aqueous batteries have a relatively small thermodynamic window (1.23V) due to the hydrogen evolution reaction in reducing environments and the oxygen evolution reaction in oxidizing environments.⁸ In contrast, nonaqueous redox flow batteries (NARFBs) have a larger operating potential window (e.g., ~5V in acetonitrile), increasing the diversity of potential redox-active molecules, and enabling higher power densities as a result of larger attainable open circuit voltages (OCV).⁹

Scheme 1. (A) Redox flow battery where A stands for anolyte (the redox-active species that undergoes reduction upon charging), and C stands for catholyte (the redox-active species that undergoes oxidation upon charging). (B) Anion exchange membrane impeding positively charged redox-active species from crossing over.



Between the two electrodes is a membrane or a separator, that functions to isolate the anolyte from the catholyte, preventing mixing (via crossover) of the redox-active molecules.¹⁰ Crossover can occur through several mechanisms, including diffusion, osmosis, electroosmosis, and migration. Several membrane types have been used in RFBs, including polymers of intrinsic microporosity (PIMs), porous separators, ion-exchange membranes, and ceramic membranes.¹¹ Each type of membrane or separator caters to a specific system. For example, PIMs offer size exclusion, which is advantageous when working with oligomeric or polymeric redox-active materials.^{12,13} Porous separators such as Daramic® or Celgard®, have been frequently used in NARFBs due to their relatively high ionic conductivity, which enables battery cycling at higher current densities.^{14,15,16} However, this improved conductivity comes at the expense of high crossover rates, especially with small redox-active species. The result is lower coulombic efficiencies and lifetimes of the battery.

One method to decrease crossover is to use a pre-mixed flow cell wherein equal quantities of anolyte and catholyte are dissolved in each reservoir^{17,18}, but doing so effectively wastes half of the redox-active materials. Additionally, there will still be a concentration gradient of the charged species across the cell during cycling, so crossover may still occur, and coulombic efficiency will suffer. A technologically relevant battery (i.e., a battery with high capacity, energy density, and energy efficiency) will be non-symmetric and have a membrane that is both highly conductive and prevents crossover.

Commercial ion-exchange membranes were originally fabricated for aqueous systems, such as fuel cells, water purification, desalination, dialysis, and/or aqueous RFBs.^{19,20,21} Specifically, anion exchange membranes (AEMs) are cross-linked polymers, assembled into three-dimensional networks with fixed, ionic functional groups (i.e., $-\text{NH}_3^+$, $-\text{NR}_2\text{H}^+$, $-\text{NR}_2\text{H}^+$, $-\text{NR}_3^+$, and $-\text{SR}_2^+$).¹⁹ AEMs should repel positively charged molecules, ensuring that cationic molecules stay in their respective tank.²² In AEMs, only anionic supporting electrolyte ions, like PF_6^- or BF_4^- , can traverse the membrane for charge balancing during charging and discharging (Scheme 1B). AEMs have been used in nonaqueous, inorganic redox flow batteries for decades^{23,24,25,26} but have more recently been adopted in nonaqueous organic redox flow batteries. For instance, Sanford and coworkers used an AEM in organic NARFBs (Fumasep FAP-375-PP) to mitigate the crossover of redox-active cyclopropenium species.^{12,27,28,29} Increasing charge incorporation and molecular size decreased the rate of crossover, with a tetramer ($4+$

charge) crossing over so slowly it was below the limit of detection within the timeframe of their experiment. As a result, FAP-375-PP has been the go-to commercial membrane in many nonaqueous redox flow battery studies,^{30,31,32,33} enabling non-symmetric small-molecule batteries. However, FAP-375-PP has recently been discontinued by the manufacturer.

To date, a systematic study has not directly compared AEMs,^{30,34,35,36,37,38,39} so it is unclear what membranes would perform best in flow battery systems. To address this limitation, we evaluated herein 26 AEMs (Table 1) for structural stability in electrochemically relevant organic solvents. From these results, seven membranes were selected for further evaluation, including measuring crossover rates, ionic conductivities, and performance in a redox flow battery. Overall, these data reveal that most commercial AEMs do not perform satisfactorily in lab-scale NARFBs. Moving forward, we suggest that researchers developing new membranes and/or evaluating new commercial membranes utilize the standard protocol described herein for benchmarking and comparison.

Table 1. Commercial anion exchange membranes evaluated. (Color blocks indicate different manufacturers of AEMs.)

Fumasep		Sustainion
FAP-330	FAB-PK-130	E30-50, T
FAPQ-330	FAD-55	E28-50, T
FAP-450	FAS-30	B22-50, T
FAA-3-30	FAS-50	X37-50, RT
FAA-3-50	FAP-330-PE	X37-50, T
FAPQ-375-PP	FAD-PET-75	PiperION
FAA-3-PK-75	FAS-PET-75	15 μm PTFE
FAA-3-PK-130	AMI-7001S	20 μm
FAM	AEMION+	80 μm

RESULTS AND DISCUSSION

Most commercial anion exchange membranes dissolve or deform in nonaqueous solvents. All membranes were first pre-treated in a saturated, aqueous solution of potassium hexafluorophosphate (KPF_6) to exchange the mobile counterions in the polymer resin with PF_6^- anions to match the supporting electrolyte used in crossover and battery studies (see SI for examples with NH_4PF_6 pretreatment). After drying, the membranes were cut into small rectangles for further analysis. To qualitatively assess the membrane's structural stability, the AEMs were soaked in neat organic solvent (MeCN, PC, DMF, DMA, and DME, separately) for 48 h to simulate long-term cycling conditions. Every membrane deformed in DMF and DMA, either dissolving completely or swelling excessively after soaking, even those with mechanical reinforcements (i.e., a polymer support). Too much swelling will immediately allow redox species to crossover the membrane.^{11,40} In contrast, many membranes remained intact in DME, but some turned opaque, which is

likely caused by a change in polymer properties (e.g., solubility). Photos of all ion-exchanged AEMs, before and after soaking in organic solvents, are included in the supporting information (SI section III).

Both MeCN and PC were chosen as the organic solvents for subsequent studies due to the incompatibility of AEMs in DMF and DMA, and the low relative permittivity of DME.⁴¹ Additionally, PC and MeCN are the two most widely used solvents in the NARFB field. Acetonitrile is an ideal organic solvent in NARFBs because of its large electrochemical window and high dielectric permittivity. Propylene carbonate is considered a green solvent because of its low relative toxicity and environmental impact, making it attractive for commercial applications.⁴² However, PC does have some drawbacks, such as a higher viscosity and lower conductivity than comparable electrolytes in MeCN. Among the 26 commercial anion exchange membranes examined, only seven demonstrated stability (no dissolution or deformation) in MeCN and PC: FAP-330, FAPQ-330, FAP-450, FAPQ-375-PP, FAP-330-PE, FAM, and AMI-7001S. These membranes were analyzed for increases in length, width, thickness, and mass to measure swelling from solvent uptake (see Section III of the SI). Interestingly, of the three membranes that swelled the least in MeCN and PC, only one (FAM) included a mechanical support (a polypropylene mesh). These results suggest that these mechanical reinforcements do not prevent swelling in nonaqueous solvents (see SI Figure S4).

Too much membrane swelling leads to higher permeability. Crossover rates were measured for three different redox-active small molecules with increasing positive charges: neutral ferrocene (Fc, catholyte), monocationic (1⁺) ammonium-appended ferrocene (FcNPF₆, catholyte), and dicationic (2⁺) butyl viologen (BuV2PF₆, anolyte) (Figure 1A). These molecules were chosen because they are electrochemically stable to galvanostatic cycling and are commercially available or easily synthesized. Additionally, these molecules have similar hydrodynamic radii (molecular size in solution),⁴³ so conclusions regarding crossover rates can be made primarily based on charge interactions with the positively charged membrane instead of size-exclusion. An H-cell was used for crossover studies,⁴⁴ enabling a membrane to sit between two half cells: one, the retentate, is composed of 25 mM redox-active material in supporting electrolyte and solvent (either 0.5 M KPF₆ in MeCN or 0.1 M KPF₆ in PC) and the other, the permeate, only contains supporting electrolyte in solvent (Figure 1B). A lower concentration of supporting electrolyte was used in PC due to the low solubility of KPF₆. Note that the supporting electrolyte concentrations were adjusted so that the ionic strengths were the same in both reservoirs. Crossover was monitored by cyclic voltammetry, which relates measured peak current to the concentration of redox-active material using a three-electrode set-up on the permeate side of the H-cell. In these experiments, redox-active species diffusion through the membrane is being measured; osmosis and electroosmosis are unlikely contributors to the crossover because solvent imbalances were not observed. Though not used in this study, ultraviolet-visible (UV-Vis) and nuclear magnetic

resonance (NMR) spectroscopy are also viable methods of measuring crossover.⁴⁵

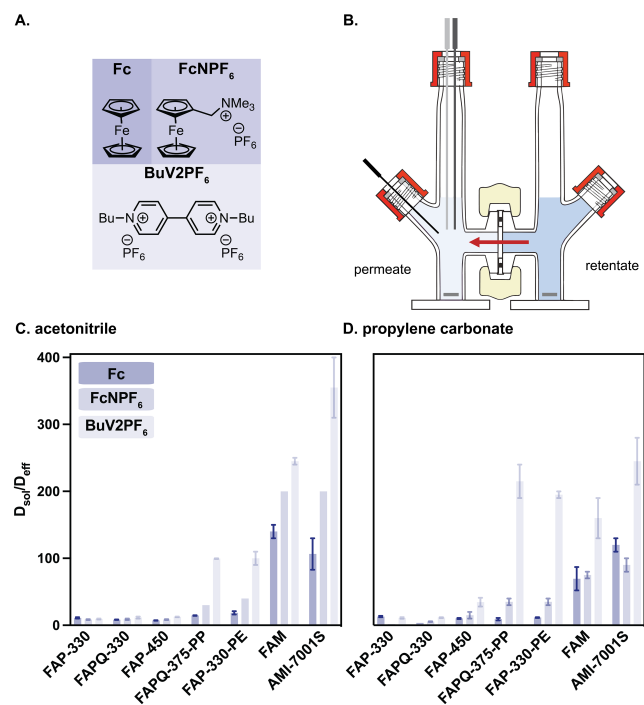


Figure 1. (A) Structures of catholytes and anolyte. (B) H-cell used for crossover experiments, adapted from Adams & Chittenden Scientific Glass Coop.⁴⁶ (C) Plot of membrane performance (D_{sol}/D_{eff}) in 0.5 M KPF₆ in MeCN. (D) Plot of membrane performance in 0.1 M KPF₆ in PC. All bars represent the average of two trials. The error bars represent the range of values.

Each membrane has a different thickness, and each molecule has a different diffusion coefficient in solution. Therefore, to compare results between membranes and molecules, we used the ratio between the redox-active molecule's diffusion coefficient in the electrolyte (D_{sol}) and its effective diffusion, or permeability, through the membrane (D_{eff}). Specifically, we used the Randles-Ševčík equation to calculate D_{sol} ^{47,48} (SI section VII) and the following equation, derived from Fick's laws of diffusion, for D_{eff} ⁴⁹ (SI section VIII):

$$D_{eff} = \frac{C_{permeate} * l * V_{permeate}}{C_0 * A}$$

$C_{permeate}$ is the initial rate of crossover (mol/s*cm³), l is the thickness of the dry membrane (cm), $V_{permeate}$ is the volume of the permeate (cm³), C_0 is the initial redox material concentration on the retentate side (mol/cm³), and A is the area of the membrane exposed to solution (cm²).

Both the absolute value and the relative values of D_{sol}/D_{eff} between molecules are important measurements. A higher absolute value of D_{sol}/D_{eff} equates to a better membrane blocking ability, whereas the relative values between the redox-active molecules studied herein reflects the membranes' selectivity for repelling positively charged molecules.¹³ We want to highlight that D_{eff} is the product of redox species diffusion through the membrane (transport) and

absorption (e.g., partitioning through the membrane), which is a thermodynamic process. Active species transport is important in flow cell cycling and can affect capacity fade, particularly in less conductive membranes, but it is not the sole contributor to permeability.

In MeCN, FAM and AMI-7001S are the best at suppressing crossover of all molecules. Both membranes display charge selectivity because they suppress the dication (BuV2PF₆) better than the monocation (FcNPF₆), and the monocation better than neutral compound (Fc) (Figure 1C). Though these two AEMs have the slowest crossover rates, they also have the lowest ionic conductivities and would therefore require a large overpotential to run in a NARFB (*vide infra*).

In PC, the most ion-selective membranes were FAPQ-375-PP and FAP-330-PE, both of which dramatically suppress the crossover of the dication compared to the monocation and neutral molecule (Figure 1D). These membranes, however, have both been discontinued from commercial suppliers. FAM and AMI-7001S also performed well comparatively but again suffered from low ionic conductivity (*vide infra*). Permeability (D_{eff}) should be no higher than 10⁻¹⁰ cm²/s and the lowest (slowest) value obtained in this work was 10⁻⁸ cm²/s for FAM and AMI-7001S in PC, a factor of 10² faster, meaning that even the best performers in our study could never be commercially viable.⁴⁰

Though we cannot attribute performance to the membranes' chemical structure, which is proprietary, we observe a "Goldilocks" correlation between solvent uptake and membrane performance in the limited data (7 membranes; Figure S4) Membranes with a high solvent uptake generally have more crossover (i.e., a smaller $D_{\text{sol}}/D_{\text{eff}}$ value.) For example, the weight of FAP-330 increased by 327% after soaking in MeCN and is a poor membrane with respect to crossover ($D_{\text{sol}}/D_{\text{eff}}$ of 9.4 for BuV2PF₆). Similarly, membranes with a low solvent uptake also showed more crossover. For example, FAPQ-330 had a mass gain of only 8% in MeCN and had an average $D_{\text{sol}}/D_{\text{eff}}$ of 11 with BuV2PF₆. In contrast, the membranes with "in between" mass gains showed the least crossover. For example, FAM and AMI-7001S exhibited a more moderate weight increase of 24% and 31%, respectively, and have the best crossover performance ($D_{\text{sol}}/D_{\text{eff}}$ of 240 and 360 for BuV2PF₆, respectively) in MeCN (SI Table S2).

AEMs with the least crossover have the lowest ionic conductivity. Anion exchange membranes should be tested in a flow battery for a more accurate comparison to grid-scale applications. As such, flow batteries were run using cationic FcNPF₆ as the catholyte and dicationic BuV2PF₆ as the anolyte, with either 0.5 M KPF₆ in MeCN or 0.1 M KPF₆ in PC. Again, the supporting electrolyte concentrations were adjusted so that the ionic strength in both reservoirs were equivalent. High ionic conductivity through the membranes is critical for AEMs in a flow cell to complete the circuit and balance charge efficiently. Ionic conductivity is an intrinsic property of membranes in supporting electrolytes, and, in our study, is measured via electrochemical impedance spectroscopy (EIS), though it could also be measured with a

four-point probe.⁵⁰ Ions can move through the membrane as solvated ions, solvent-separated ion pairs, contact ion pairs, or in aggregates. Because the batteries used low to moderate ion concentrations, and the membranes were swollen, we expect that the ions primarily move through the membranes as solvated free ions, though the other mechanisms are possible.^{51,52}

The system resistance was calculated by subtracting the bulk electrolyte resistance (measured from a blank experiment without a membrane) from the total resistance measured in the flow cell. For AEMs in nonaqueous systems, a practical ionic conductivity range is >1 mS/cm by way of the maximum area-specific resistance (ASR) for a membrane with a thickness of ~25 μm (2.3 Ω*cm²) is desired.^{53,54} None of the membranes exhibited ionic conductivities over 1 mS/cm (Table 1 and Figure S5). Membranes with high ionic conductivity and low redox-active molecule permeability are desired (Figure 2A). Unfortunately, the membranes with the highest ionic conductivities also exhibited the highest permeabilities of redox-active species (Figure 2B). These results cannot be explained by differences in swelling; (Figure S6); as an example, the least (8%) and most (327%) swollen membranes both exhibited similar ionic conductivities (317 and 390 μS/cm, respectively) and permeabilities (7.43 x 10⁻⁷ and 6.12 x 10⁻⁷ cm²/s; for BuV2PF₆ in MeCN). Overall, the data show that no membrane, solvent, or redox molecule combination was able to reach these targeted metrics, and as a result, none of the evaluated systems are suitable for NARFB applications.

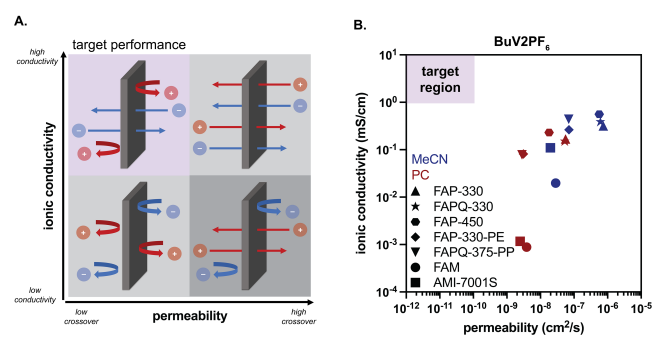


Figure 2. (A) Idealized plot of ionic conductivity of supporting electrolyte anions and permeability of redox-active cations through anion exchange membranes. (B) Plot of measured ionic conductivity and permeability of each AEM in MeCN and PC with BuV2PF₆.

Nevertheless, all seven membranes were advanced to battery testing to measure capacity fade, coulombic efficiency, and voltage efficiency, among other variables. Capacity fade measures how much redox-active material can be discharged over time, with a lower fade equating to a longer battery lifetime.⁵⁵ Coulombic efficiency is the difference between the capacities reached during charging and discharging and reflects how much of stored charge is accessible. Voltage efficiency accounts for any overpotential necessary to run the battery and dictates whether enough power is generated to be commercially viable. Ideally, a battery will have low capacity fade, high coulombic efficiency, and high

voltage efficiency. However, it can be challenging to simultaneously optimize these factors in RFBs.

In MeCN, the membranes with the lowest capacity fade and the highest coulombic efficiency were FAM and AMI-7001S (Figure 3). However, both FAM and AMI-7001S have low voltage efficiencies (34% and 21%, respectively) (Table 2), requiring considerably more energy to run the battery than the open-circuit voltage (1.05 V). In PC, the best membrane was FAP-330-PE, which had the lowest capacity fade (10% over 22 h), with a high coulombic efficiency (97%) and modest voltaic efficiency (80%).⁵⁶ Nevertheless, this membrane was discontinued and is no longer available. The capacity fade is likely due to crossover due to both diffusion and migration, which may explain why the discharge capacity surpasses 50% losses in FAP-330, FAPQ-330, and FAP-450.^{57,58} No solvent imbalances were observed, suggesting that neither osmosis nor electroosmosis contributed to crossover.

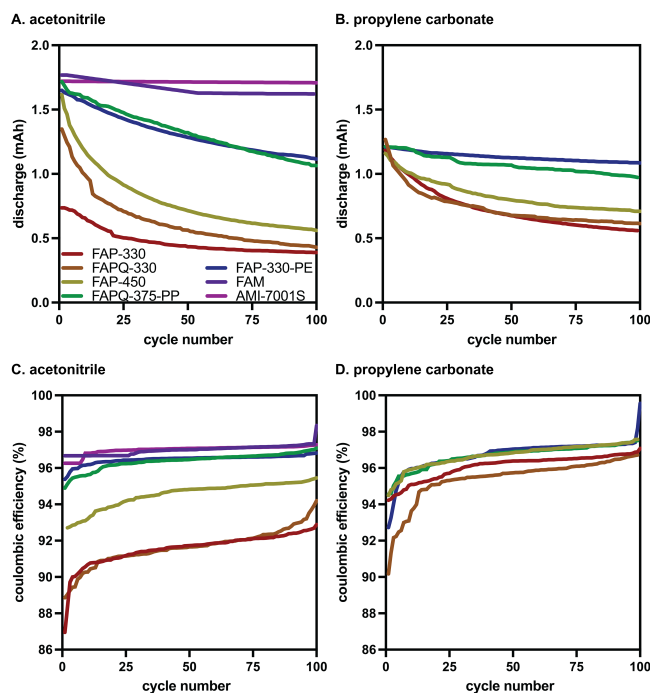


Figure 3. Capacity fade in (A) MeCN and (B) PC. Coulombic efficiency in (C) MeCN and (D) PC over 100 cycles. The theoretical capacity of the battery is 2.7 mAh.

Table 2. Dry thickness, ionic conductivity, and voltage efficiency values for AEMs in MeCN and PC.

AEM	dry thickness (μm)	MeCN	PC	MeCN	PC
		ionic conductivity ($\mu\text{S}/\text{cm}$)		voltage efficiency (%)	
FAP-330	32	317 ± 7	168 ± 4	87 ± 1	80 ± 1
FAPQ-330	36	390 ± 10	151 ± 3	90 ± 1	74 ± 1
FAP-450	56	560 ± 10	231 ± 4	95 ± 1	78 ± 1

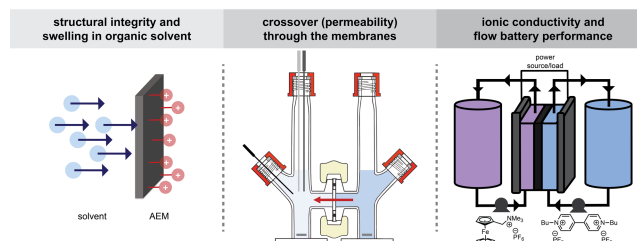
FAPQ-375-PP	107	440 ± 10	78 ± 3	90 ± 1	34 ± 1
FAP-330-PE	45	263 ± 8	81 ± 1	95 ± 1	66 ± 1
FAM	526	19.7 ± 0.03	0.88 ± 0.03	21.0 ± 0.5	n.d.
AMI-7001S	568	110 ± 3	1.17 ± 0.05	33.5 ± 0.5	n.d.

A standardized protocol is necessary to compare between commercial and synthesized membranes. If all studies use the same redox-active molecules, solvents, and supporting electrolytes for crossover and battery testing, a direct comparison can be made between different membranes. To this end, we recommend that all NARFB groups that are synthesizing their own AEMs (or evaluating new commercial membranes) use the following protocol as a baseline: (1) membrane integrity testing and swelling measurements in MeCN, PC, DMF, DMA, and DME, (2) crossover studies using Fc, FcNPF₆, and BuV2PF₆, (3) EIS to determine ionic conductivity, and (4) evaluation in flow battery cycling.

To maximize ionic conductivity of supporting electrolyte (e.g., KPF₆), we suggest using MeCN as a solvent over PC, assuming similar redox-active molecule solubility in both solvents. KPF₆ is a convenient supporting electrolyte because it has no ¹H or ¹³C signals via nuclear magnetic resonance spectroscopy, simplifying spectral analyses that may provide insight into redox-active molecule degradation. If this protocol is widely adopted, it will be easier to benchmark membranes and push the boundaries of membrane fabrication for RFBs.

Limitations and other considerations. Our workflow focuses on the membranes, and an easily translatable performance test to benchmark them. However, some conditions must be considered when adopting our methodology. Although Fc, FcNPF₆, and BuV2PF₆ are good model compounds, we recognize that crossover can also be mitigated through chemical synthesis (i.e., installing ionic functional groups onto redox molecules to be repelled by ion exchange membranes), meaning that our measured crossover rates of neutral, 1⁺, and 2⁺ species may not translate perfectly to other molecules.

Scheme 2. Recommended protocol for evaluating the performance of anion exchange membranes.



Additionally, some membrane characterization methods (i.e., ion-exchange capacity⁵⁹, swelling/sorption with different supporting electrolytes⁶⁰, and surface area/pore size of the membrane⁶¹) lie beyond the scope of this study but are important for full characterization of new membranes. Other methods to evaluate electrochemical performance and crossover *in situ* include dialysis diagnostics by Darling and coworkers, using an applied electric field⁶² and compositionally unbalanced symmetric cell cycling by Brushett and coworkers.⁶³

Furthermore, our protocol is performed at low concentrations but transport and membrane properties (i.e., conductivity, partitioning, swelling) are likely to change at application-relevant active species concentrations.⁶⁴ Battery performance depends on volume, flow rate, concentrations of redox species, viscosity, electrode area, temperature, battery cell structure, and many other parameters. With these considerations, we emphasize that this study is for membrane comparison, and the relative values between the model compounds and membranes are what enable a precise comparison.

CONCLUSIONS

Commercially available AEMs were examined as potential membranes for NARFBs. Performance was compared based on structural stability in nonaqueous solvents, swelling, crossover of the redox-active molecules, ionic conductivity of the charge-carrying ion, and a 100-cycle flow battery. Of the 26 membranes initially tested, only seven membranes emerged as good candidates for full evaluation. Overall, no commercial anion exchange membrane studied had an acceptable performance in *all* categories. Based on our data, FAPQ-375-PP and FAP-330-PE are the best membrane candidates for nonaqueous redox flow batteries in acetonitrile and only the latter membrane works well in propylene carbonate; however, these two membranes have been discontinued by the manufacturer. Consequently, new membranes (commercial or synthesized^{65,66,67,68}) are needed for NARFBs and should be evaluated using our suggested protocol to accurately benchmark them against existing membranes.

ASSOCIATED CONTENT

Supporting Information

All materials, synthetic and electrochemical procedures, structural (NMR, MS, and elemental analysis) and electrochemical characterization (crossover, CV, EIS, batteries), solvent uptake and swelling studies, and photos of all AEMs in organic solvents are provided in the supporting information. (PDF)

The Supporting Information is available free of charge on the ACS Publications website.

AUTHOR INFORMATION

Corresponding Author

*Anne J. McNeil – Department of Chemistry and Macromolecular Science and Engineering Program, University of Michigan,

Ann Arbor, Michigan 48109-1055, United States; orcid.org/0000-0003-4591-3308; Email: ajmneil@umich.edu

*Shelley D. Minteer – Department of Chemistry, Missouri University of Science and Technology, Rolla, Missouri, 65409-6518, United States; orcid.org/0000-0002-5788-2249; Email: shelley.minteer@mst.edu

ORCID

Jessica L. Tami 0000-0003-3106-5790

Motiur Mazumder 0000-0002-3095-3019

Anne J. McNeil 0000-0003-4591-3308

Shelley D. Minteer 0000-0002-5788-2249

Author Contributions

CRedit: **Jessica L. Tami** contributed to conceptualization (equal), data curation (equal), formal analysis (equal), methodology (equal), visualization (lead), writing original draft (lead), and writing review & editing (lead). **Md. Motiur R. Mazumder** contributed to conceptualization (equal), data curation (equal), formal analysis (equal), and methodology (equal). **Grace E. Cook** contributed to data curation and methodology. **Shelley D. Minteer** contributed to conceptualization, funding acquisition, investigation, project administration, resources, supervision, and writing review & editing. **Anne J. McNeil** contributed to conceptualization, funding acquisition, investigation, project administration, resources, supervision, and writing review & editing.

Funding Sources

This research was supported by the Department of Energy through the Joint Center for Energy Storage Research (JCESR), an Energy Innovation Hub funded by the U.S. Department of Energy, Office of Science, Basic Energy Sciences.

ACKNOWLEDGMENT

J.L.T., M.M.R.M., A.J.M. and S.D.M. gratefully acknowledge support and helpful conversations from the Joint Center for Energy Storage Research.

ABBREVIATIONS

AEM, anion exchange membrane; Fc, ferrocene; RFB, redox flow battery; NARFB, nonaqueous redox flow battery; MeCN, acetonitrile; PC, propylene carbonate; DMF, *N,N*-dimethylformamide; DMA, *N,N*-dimethylacetamide; DME, dimethoxyethane; ASR, area specific resistance; NMR, nuclear magnetic resonance spectroscopy; UV-Vis, ultraviolet-Visible spectroscopy; OCV, open circuit voltage; EIS, electrochemical impedance spectroscopy.

REFERENCES

- ¹Ziegler, M. S.; Mueller, J. M.; Pereira, G. D.; Song, J.; Ferrara, M.; Chiang, Y.-M.; Trancik, J. E. Storage Requirements and Costs of Shaping Renewable Energy Toward Grid Decarbonization. *Joule* **2019**, *3*, 2134–2153.
- ²Sánchez-Díez, E.; Ventosa, E.; Guarnieri, M.; Trovò, A.; Flox, C.; Marcilla, R.; Soavi, F.; Mazur, P.; Aranzabe, E.; Ferret, R. Redox Flow Batteries: Status and Perspective Towards Sustainable Stationary Energy Storage. *J. Power Sources* **2021**, *481*, 228804.
- ³Noack, J.; Roznyatovskaya, N.; Herr, T.; Fischer, P. The Chemistry of Redox-Flow Batteries. *Angew. Chem. Int. Ed.* **2015**, *54*, 9776–9809.
- ⁴Arévalo-Cid, P.; Dias, P.; Mendes, A.; Azevedo, J. Redox Flow Batteries: A New Frontier on Energy Storage. *Sustainable Energy Fuels* **2021**, *5*, 5366–5419.
- ⁵Choi, C.; Kim, S.; Kim, R.; Choi, Y.; Kim, S.; Jung, H.; Yang, J. H.; Kim, H.-T. A Review of Vanadium Electrolytes for Vanadium Redox Flow Batteries. *Renew. Sustain. Energy Rev.* **2017**, *69*, 263–274.
- ⁶Lourenssen, K.; Williams, J.; Ahmadpour, F.; Clemmer, R.; Tasnim, S. Vanadium Redox Flow Batteries: A Comprehensive Review. *J. Energy Storage* **2019**, *25*, 100844.
- ⁷Cunha, Á.; Martins, J.; Rodrigues, N.; Brito, F. P. Vanadium Redox Flow Batteries: A Technology Review. *Int. J. Energy Res.* **2014**, *39*, 889–918.
- ⁸Kühnel, R.-S.; Reber, D.; Battaglia, C. Perspective—Electrochemical Stability of Water-in-Salt Electrolytes. *J. Electrochem. Soc.* **2020**, *167*, 070544.
- ⁹Li, M.; Rhodes, Z.; Cabrera-Pardo, J.; Minter, S. D. Recent Advancements in Rational Design of Non-Aqueous Organic Redox Flow Batteries. *Sustain. Energy Fuels* **2020**, *4*, 4370–4389.
- ¹⁰Huang, Y.; Gu, S.; Yan, Y.; Fong Yau Li, S. Nonaqueous Redox-Flow Batteries: Features, Challenges, and Prospects. *Curr. Opin. Chem. Eng.* **2015**, *8*, 105–113.
- ¹¹Yuan, J.; Pan, Z.-Z.; Jin, Y.; Qui, Q.; Zhang, C.; Zhao, Y.; Li, Y. Membranes in Non-Aqueous Redox Flow Battery: A Review. *J. Power Sources* **2021**, *500*, 229983.
- ¹²Hendriks, K. H.; Robinson, S. G.; Braten, M. N.; Sevov, C. S.; Helms, B. A.; Sigman, M. S.; Minter, S. D.; Sanford, M. S. High-Performance Oligomeric Catholytes for Effective Macromolecular Separation in Nonaqueous Redox Flow Batteries. *ACS Cent. Sci.* **2018**, *4*, 189–196.
- ¹³Doris, S. E.; Ward, A. L.; Baskin, A.; Frischmann, P. D.; Gavvalapalli, N.; Chénard, E.; Sevov, C. S.; Prendergast, D.; Moore, J. S.; Helms, B. A. Macromolecular Design Strategies for Preventing Active-Material Crossover in Non-Aqueous All-Organic Redox-Flow Batteries. *Angew. Chem. Int. Ed.* **2017**, *56*, 1595–1599.
- ¹⁴De La Garza, G. D.; Preet Kaur, A.; Shkrob, I. A.; Robertson, L. A.; Odom, S. A.; McNeil, A. J. Soluble and Stable Symmetric Tetrazines as Anolytes in Redox Flow Batteries. *J. Mat. Chem. A*, **2022**, *10*, 18745–18752.
- ¹⁵Kim, D.; Sanford, M. S.; Vaid, T. P.; McNeil, A. J. A Nonaqueous Redox-Matched Flow Battery with Charge Storage in Insoluble Polymer Beads. *Chem. Eur. J.* **2022**, *28*, e202200149.
- ¹⁶Nagarjuna, G.; Hui, J.; Cheng, K. J.; Lichtenstein, T.; Shen, M.; Moore, J. S.; Rodríguez-López, J. Impact of Redox-Active Polymer Molecular Weight on the Electrochemical Properties and Transport Across Porous Separators in Nonaqueous Solvents. *J. Am. Chem. Soc.* **2014**, *136*, 16309–16316.
- ¹⁷Duan, W.; Huang, J.; Kowalski, J. A.; Shkrob, I. A.; Vijayakumar, M.; Walter, E.; Pan, B.; Yang, Z.; Milshtein, J. D.; Li, B.; Liao, C.; Zhang, Z.; Wang, W.; Liu, J.; Moore, J. S.; Brushett, F. R.; Zhang, L.; Wei, X. “Wine-Dark Sea” in an Organic Flow Battery: Storing Negative Charge in 2,1,3-Benzothiadiazole Radicals Leads to Improved Cyclability. *ACS Energy Lett.* **2017**, *2*, 1156–1161.
- ¹⁸Wei, X.; Duan, W.; Huang, J.; Zhang, L.; Li, B.; Reed, D.; Xu, W.; Sprenkle, V.; Wang, W. A High-Current, Stable Nonaqueous Organic Redox Flow Battery. *ACS Energy Lett.* **2016**, *1*, 705–711.
- ¹⁹You, W.; Noonan, K. J. T.; Coates, G. W. Alkaline-Stable Anion Exchange Membranes: A Review of Synthetic Approaches. *Prog. Polym. Sci.* **2020**, *100*, 101177.
- ²⁰Zeng, L.; Zhao, T. S.; Wei, L.; Jiang, H. R.; Wu, M. C. Anion Exchange Membranes for Aqueous Acid-Based Redox Flow Batteries: Current Status and Challenges. *Appl. Energy* **2019**, *233–234*, 622–643.
- ²¹Du, N.; Roy, C.; Peach, R.; Turnbull, M.; Thiele, S.; Bock, C. Anion-Exchange Membrane Water Electrolyzers. *Chem. Rev.* **2022**, *122*, 11830–11895.
- ²²Jett, B.; Flynn, A.; Sigman, M. S.; Sanford, M. S. Identifying structure-function relationships to modulate crossover in nonaqueous redox flow batteries. *J. Mater. Chem. A* **2023**, *11*, 22288–22294.
- ²³Matsuda, Y.; Tanaka, K.; Okada, M.; Takasu, Y.; Morita, M.; Matsumura-Inoue, T. A Rechargeable Redox Battery Utilizing Ruthenium Complexes with Non-Aqueous Organic Electrolyte. *J. Appl. Electrochem.* **1988**, *18*, 909–914.
- ²⁴Liu, Q.; Sleightholme, A. E. S.; Shinkle, A. A.; Li, Y.; Thompson, L. T. Non-Aqueous Vanadium Acetylacetonate Electrolyte for Redox Flow Batteries. *Electrochem. Comm.* **2009**, *11*, 2312–2315.
- ²⁵Mun, J.; Lee, M.-J.; Park, J.-W.; Oh, D.-J.; Lee, D.-Y.; Doo, S.-G. Non-Aqueous Redox Flow Batteries with Nickel and Iron Tris(2,2'-Bipyridine) Complex Electrolyte. *Electrochem. Solid-State Lett.* **2012**, *15*, A80.
- ²⁶Shin, S.-H.; Yun, S.-H.; Moon, S.-H. A Review of Current Developments in Non-Aqueous Redox Flow Batteries: Characterization of Their Membranes for Design Perspective. *RSC Adv.* **2013**, *3*, 9095–9116.
- ²⁷Robinson, S. G.; Yan, Y.; Hendriks, K. H.; Sanford, M. S.; Sigman, M. S. Developing a Predictive Solubility Model for Monomeric and Oligomeric Cyclopropenium-Based Flow Battery Catholytes. *J. Am. Chem. Soc.* **2019**, *141*, 10171–10176.

- ²⁸Shrestha, A.; Hendricks, K. H.; Sigman, M. S.; Minter, S. D.; Sanford, M. S. Realization of an Asymmetric Non-Aqueous Redox Flow Battery through Molecular Design to Minimize Active Species Crossover and Decomposition. *Chem. Eur. J.* **2020**, *26*, 5369–5373.
- ²⁹Yan, Y.; Robinson, S. G.; Sigman, M. S.; Sanford, M. S. Mechanism-Based Design of a High-Potential Catholyte Enables a 3.2 V All-Organic Nonaqueous Redox Flow Battery. *J. Am. Chem. Soc.* **2019**, *141*, 15301–15306.
- ³⁰Montoto, E. C.; Nagarjuna, G.; Moore, J. S.; Rodríguez-López, J. Redox Active Polymers for Non-Aqueous Redox Flow Batteries: Validation of the Size-Exclusion Approach. *J. Electrochem. Soc.* **2017**, *164*, A1688.
- ³¹Yan, Y.; Sitala, P.; Odom, S. A.; Vaid, T. P. High Energy Density, Asymmetric, Nonaqueous Redox Flow Batteries without a Supporting Electrolyte. *ACS Appl. Mater. Interfaces* **2022**, *14*, 49633–49640.
- ³²Ahn, S.; Jang, H. H.; Kang, J.; Na, M.; Seo, J.; Singh, V.; Joo, J. M.; Byon, H. R. Systematic Designs of Dicationic Heteroarylpyridiniums as Negolytes for Nonaqueous Redox Flow Batteries. *ACS Energy Lett.* **2021**, *6*, 3390–3397.
- ³³Daub, N.; Hendricks, K. H.; Janssen, R. A. J. Two-Electron Tetrathiafulvalene Catholytes for Nonaqueous Redox Flow Batteries. *Batteries & Supercaps* **2022**, *5*, e202200386.
- ³⁴Krivina, R. A.; Lindquist, G. A.; Yang, M. C.; Cook, A. K.; Hendon, C. H.; Motz, A. R.; Capuano, C.; Ayers, K. E.; Hutchinson, J. E.; Boettcher, S. W. Three-Electrode Study of Electrochemical Ionomer Degradation Relevant to Anion-Exchange-Membrane Water Electrolyzers. *ACS Appl. Mater. Interfaces* **2022**, *14*, 18261–18274.
- ³⁵Hudak, N. S.; Small, L. J.; Pratt, H. D.; Anderson, T. M. Through-Plane Conductivities of Membranes for Nonaqueous Redox Flow Batteries. *J. Electrochem. Soc.* **2015**, *162*, A2188–A2194.
- ³⁶Liang, Z.; Attanayake, N. H.; Greco, K. V.; Neyhouse, B. J.; Barton, J. L.; Kaur, A. P.; Eubanks, W. L.; Brushett, F. R.; Landon, J.; Odom, S. A. Comparison of Separators vs Membranes in Nonaqueous Redox Flow Battery Electrolytes Containing Small Molecule Active Materials. *ACS Appl. Energy Mater.* **2021**, *4*, 5443–5451.
- ³⁷Mushtaq, K.; Lagarteria, T.; Zaidi, A. A.; Mendes, A. *In-Situ* Crossover Diagnostics to Assess Membrane Efficacy for Non-Aqueous Redox Flow Battery. *J. Energy Storage* **2021**, *40*, 102713.
- ³⁸George, T. Y.; Thomas, I. C.; Haya, N. O.; Deneen, J. P.; Wang, C.; Aziz, M. J. Membrane-Electrolyte System Approach to Understanding Ionic Conductivity and Crossover in Alkaline Flow Cells. *ACS Appl. Mater. Interfaces* **2023**, *15*, 57252–57264.
- ³⁹Cassady, H. J.; Yang, Z.; Rochow, M. F.; Saraidaridis, J. D.; Hickner, M. A. Crossover Flux and Ionic Resistance Metrics in Polysulfide-Permanganate Redox Flow Battery Membranes. *J. Electrochem. Soc.*, **2024**, *171*, 030527.
- ⁴⁰Lehmann, M. L.; Tyler, L.; Self, E. C.; Yang, G.; Nanda, J.; Saito, T. Membrane Design for Non-Aqueous Redox Flow Batteries: Current Status and Path Forward. *Chem* **2022**, *8*, 1611–1636.
- ⁴¹Gong, K.; Fang, Q.; Gu, S.; Li, S. F. Y.; Yan, Y. Nonaqueous Redox-Flow Batteries: Organic Solvents, Supporting Electrolytes, and Redox Pairs. *Energy Environ. Sci.* **2015**, *8*, 3515–3530.
- ⁴²Alder, C. M.; Hayler, J. D.; Henderson, R. K.; Redman, A. M.; Shukla, L.; Shuster, L. E.; Sneddon, H. F. Updating and Further Expanding GSK's Solvent Sustainability Guide. *Green Chem.* **2016**, *18*, 3879–3890.
- ⁴³The hydrodynamic radii are approximated with the Stokes-Einstein equation, wherein the radius is inversely proportional to the diffusion coefficient of the molecule in solution (diffusion coefficients are calculated in SI Table S8) and solution viscosity, which is primarily affected by the solvent and excess supporting electrolyte. See ref: Berkowicz, S.; Perakis, F. Exploring the Validity of the Stokes-Einstein Relation in Supercooled Water Using Nanomolecular Probes. *Phys. Chem. Chem. Phys.* **2021**, *23*, 25490.
- ⁴⁴Li, M.; Odom, S. A.; Pancoast, A. R.; Robertson, L. A.; Vaid, T. P.; Agarwal, G.; Doan, H. A.; Wang, Y.; Suduwella, T. M.; Bheemireddy, S. R.; Ewoldt, R. H.; Assary, R. S.; Zhang, L.; Sigman, M. S.; Minter, S. D. Experimental Protocols for Studying Organic Non-Aqueous Redox Flow Batteries. *ACS Energy Lett.* **2021**, *6*, 3932–3943.
- ⁴⁵Gandomi, Y. A.; Aaron, D. S.; Houser, J. R.; Daugherty, M. C.; Clement, J. T.; Pezeshki, A. M.; Ertugrul, T. Y.; Moseley, D. P.; Mench, M. M. Critical Review—Experimental Diagnostics and Material Characterization Techniques Used on Redox Flow Batteries. *J. Electrochem. Soc.* **2018**, *165*, A970.
- ⁴⁶Adams & Chittenden Scientific Glass Coop Home Page. <https://adamschittenden.com/> (accessed 2024/02/09).
- ⁴⁷A. J. Bard and L. R. Faulkner, *Electrochemical Methods: Fundamentals and Applications*; Harris, D.; Swain, E.; Robey C.; Aiello, E., John Wiley and Sons, INC.: US, 2001; pp. 230–243.
- ⁴⁸Wang, H.; Sayed, S. Y.; Lubner, E. J.; Olsen, B. C.; Shirurkar, S. M.; Venkatakrishnan, S.; Tefashe, U. M.; Farquhar, A. K.; Smotkin, E. S.; McCreery, R. L.; Buriak, J. M. Redox Flow Batteries: How to Determine Electrochemical Kinetic Parameters. *ACS Nano* **2020**, *14*, 2575–2584.
- ⁴⁹Yang, Z.; Tong, L.; Tabor, D. P.; Beh, E. S.; Goulet, M.-A.; De Porcellinis, D.; Aspuru-Guzik, A.; Gordon, R. G.; Aziz, M. J. Alkaline Benzoquinone Aqueous Flow Battery for Large-Scale Storage of Electrical Energy. *Adv. Energy Mater.* **2018**, *8*, 1702056.
- ⁵⁰Díaz, J. C.; Kitto, D.; Kamcev, J. Accurately Measuring the Ionic Conductivity of Membranes via the Direct Contact Method. *J. Membr. Sci.* **2023**, *669*, 121304.
- ⁵¹Fong, K. D.; Self, J.; Diederichsen, K. M.; Wood, B. M.; McCloskey, B. D.; Persson, K. A. Ion transport and the true transference number in nonaqueous polyelectrolyte solutions for lithium-ion batteries. *ACS Cent. Sci.* **2019**, *5*, 1250–1260.
- ⁵²Ford, H. O.; Park, B.; Jiang, J.; Seidler, M. E.; Schaefer, J. L. Enhanced Li⁺ conduction within single-ion conducting polymer gel electrolytes via reduced cation-polymer interaction. *ACS Materials Lett.* **2020**, *2*, 272–279.
- ⁵³Su, L.; Darling, R. M.; Gallager, K. G.; Xie, W.; Thelen, J. L.; Badel, A. F.; Barton, J. L.; Cheng, K. J.; Balsara, N. P.; Moore, J. S.; Brushett, F. R. An Investigation of the Ionic

Conductivity and Species Crossover of Lithiated Nafion 117 in Nonaqueous Electrolytes. *J. Electrochem. Soc.* **2016**, *163*, A5253.

⁵⁴Darling, R.; Gallaher, K.; Xie, W.; Su, L.; Brushett, F. Transport Property Requirements for Flow Battery Separators. *J. Electrochem. Soc.* **2016**, *163*, A5029.

⁵⁵Kong, T.; Li, J.; Wang, W.; Zhou, X.; Xie, Y.; Ma, J.; Li, X.; Wang, Y. Enabling Long-Life Aqueous Organic Redox Flow Batteries with a Highly Stable, Low Redox Potential Phenazine Anolyte. *ACS Appl. Mater. Interfaces* **2024**, *16*, 752–760.

⁵⁶Modak, S. V.; Shen, W.; Singh, S.; Herrera, D.; Oudeif, F.; Goldsmith, B. R.; Huan, X.; Kwabi, D. G. Understanding Capacity Fade in Organic Redox-Flow Batteries by Combining Spectroscopy with Statistical Inference Techniques. *Nat. Commun.* **2023**, *14*, 3602.

⁵⁷Small, L. J.; Pratt III, H. D.; Anderson, T. M. Crossover in membranes for aqueous soluble organic redox flow batteries. *J. Electrochem. Soc.* **2019**, *166*, A2536.

⁵⁸Neyhouse, B. J.; Brushett, F. R. A spreadsheet-based redox flow battery cell cycling model enabled by closed-form approximations. *J. Electrochem. Soc.* **2024**, *171*, 080518.

⁵⁹Jacquemond, R. R.; Geveling, R.; Forner-Cuenca, A.; Nijmeijer, K. On the Characterization of Membrane Transport Phenomena and Ion Exchange Capacity for Non-Aqueous Redox Flow Batteries. *J. Electrochem. Soc.* **2022**, *169*, 080528.

⁶⁰Geise, G. M.; Paul, D. R.; Freeman, B. D. Fundamental Water and Salt Transport Properties of Polymeric Materials. *Prog. Polym. Sci.* **2014**, *39*, 1–42.

⁶¹Machado, C. A.; Brown, G. O.; Yang, R.; Hopkins, T. E.; Pribyl, J. G.; Epps, T. H. Redox Flow Battery Membranes: Improving Battery Performance by Leveraging Structure–Property Relationships. *ACS Energy Lett.* **2021**, *6*, 158–176.

⁶²Darling, R. M.; Saraidaridis, J. D.; Shovlin, C.; Fortin, M. The Influence of Current Density on Transport of Vanadium Acetylacetonate through a Cation-Exchange Membrane. *J. Electrochem. Soc.* **2022**, *169*, 030514.

⁶³Neyhouse, B. J.; Darling, R. M.; Saraidaridis, J. D.; Brushett, F. R. A Method for Quantifying Crossover in Re-

dox Flow Cells through Compositionally Unbalanced Symmetric Cell Cycling. *J. Electrochem. Soc.* **2023**, *170*, 080514.

⁶⁴Fenton, Jr., A. M.; Kant Jha, R.; Neyhouse, B. J.; Preet Kaur, A.; Dailey, D. A.; Odom, S. A.; Brushett, F. R. On the Challenges of Materials and Electrochemical Characterization of Concentrated Electrolytes for Redox Flow Batteries. *J. Mater. Chem. A* **2022**, *10*, 17988.

⁶⁵Peltier, C. R.; Rhodes, Z.; Macbeth, A. J.; Milam, A.; Carroll, E.; Coates, G. W.; Minteer, S. D. Suppressing Crossover in Nonaqueous Redox Flow Batteries with Polyethylene-Based Anion-Exchange Membranes. *ACS Energy Lett.* **2022**, *7*, 4118–4128.

⁶⁶Mazumder, M. R.; Jadhav, R. G.; Minteer, S. D. Phenyl Acrylate-Based Cross-Linked Anion Exchange Membranes for Non-Aqueous Redox Flow Batteries. *ACS Mater. Au* **2023**, *3*, 557–568.

⁶⁷Li, Y.; Sniekers, J.; Malaquias, J.C.; Van Goethem, C.; Binnemans, K.; Fransaer, J.; Vankelecom, I. F. J. Cross-linked Anion Exchange Membranes Prepared from Poly(phenylene oxide) (PPO) for Non-Aqueous Redox Flow Batteries. *J. Power Sources* **2018**, *378*, 338–344.

⁶⁸Mandal, M.; Huang, G.; Hassan, N. U.; Mustain, W. E.; Kohl, P. A. Poly(norbornene) Anion Conductive Membranes: Homopolymer, Block Copolymer and Random Copolymer Properties and Performance. *J. Mater. Chem A* **2020**, *8*, 17568–17578.

TOC Graphic

